

# Tamaththul3D: High-Fidelity 3D Saudi Sign Language Avatars from Monocular Video

Eyad Alghamdi, Sattam Altuuaim, Obay Ghulam, Abdulrahman Qutah, Yousef Basoodan  
University of Jeddah, Jeddah, Saudi Arabia

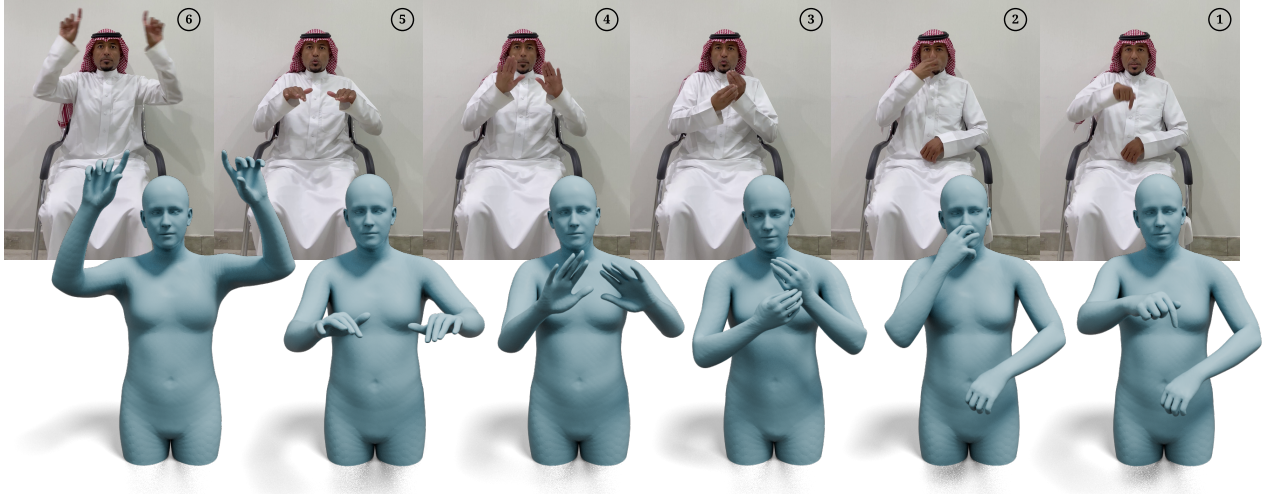


Fig. 1: Tamaththul3D: From monocular video of Saudi Sign Language (top) to reconstructed 3D avatars with detailed hand and body pose (bottom). Our method captures the intricate finger articulations and body movements essential for sign language communication.

**Abstract**—Arabic Sign Language (ArSL) and its dialects serve approximately 400 million Arabic speakers worldwide, yet the community lacks high-quality 3D parametric annotations and specialized reconstruction methods for avatar generation. We address this critical gap through two key contributions: First, we introduce the first high-quality 3D parametric annotations for the Ishara-500 Saudi Sign Language dataset, providing precise SMPL-X parameters for 500 culturally authentic SSL signs. Second, we present Tamaththul3D, a specialized reconstruction pipeline designed for ArSL’s unique articulation patterns. Our pipeline integrates SMPLer-X for robust body estimation, WiLoR for detailed hand refinement with automatic localization and mirroring, and MediaPipe for 2D pose supervision. Through kinematic-chain-based wrist alignment with hybrid swing-twist decomposition and 2D-supervised joint optimization, Tamaththul3D achieves state-of-the-art hand accuracy (up to 32% improvement over previous methods) while maintaining competitive body pose. Together, these 3D annotations and Tamaththul3D pipeline establish the first comprehensive framework for high-fidelity ArSL avatar reconstruction, enabling new accessibility technologies and cultural preservation efforts for the Arab Deaf community.

## I. INTRODUCTION

Arabic Sign Language (ArSL) and its regional variants, like Saudi Sign Language (SSL), serve as the primary communication systems for Deaf communities throughout the Arab world. The World Federation of the Deaf [27] highlights the global importance of sign languages for deaf communities. For the Arab region specifically, hard numbers are scarce, but the

World Health Organization notes that a significant population in the Middle East and Africa has hearing loss [28]—many of whom depend on sign languages for daily communication. Recent years have seen major progress in 3D human pose estimation and avatar reconstruction [20], [3], [14], [18], yet there’s still no specialized system for creating detailed 3D signing avatars from ArSL videos with accurate parametric annotations.

This missing piece severely limits progress in building educational tools, improving telecommunication access, and preserving cultural heritage for Arab Deaf communities. Alyami et al. [1] recently released Ishara-500, a large 2D dataset for Saudi Sign Language. However, existing ArSL datasets [17], [26] lack 3D parametric annotations, which blocks the development of avatar-based applications. While Western sign language datasets like WLASL [13] and PHOENIX-2014 [10] have driven advances in recognition, no comparable 3D resources exist for ArSL.

**Unique Challenges of ArSL.** Sign language reconstruction presents distinct challenges compared to general human pose estimation [29]. First, hand articulation complexity: sign languages convey meaning through precise finger configurations, palm orientations, and rapid hand motions. General-purpose pose estimation methods [20], [14] often fail to capture these intricate details that render signs incomprehensible. Second, cultural specificity: different sign languages have unique grammatical structures, signing spaces, and gestural patterns. ArSL

exhibits distinct characteristics in hand shapes and movement patterns that differ from American Sign Language (ASL) or British Sign Language (BSL). Third, multi-modal integration: effective signing requires simultaneous capture of hand pose, body orientation, and facial expressions, all of which contribute to semantic meaning.

**Limitations of Existing Approaches.** Existing sign language avatar reconstruction methods [7], [2] have several shortcomings. SGNify [7] uses linguistic priors but produces visually incorrect hand gestures. Neural Sign Actors [2] focuses on generating sign language from text and developed a curation process for SMPL-X datasets using OSX [14] and MediaPipe [16]. DexAvatar [12] uses sign-language-aware priors for optimization-based reconstruction. However, all existing methods are developed and tested only on Western sign languages, particularly ASL and German Sign Language, with no work on ArSL.

**Contributions:** We introduce **Tamaththul3D** (from Arabic تمثيل, meaning “representation” or “likeness”), the first comprehensive pipeline specifically designed for Saudi/Arabic Sign Language avatar reconstruction. Our key innovation is a hybrid approach that combines geometric inverse kinematics for forearm alignment with optimization-based shoulder refinement. We leverage SMPLer-X [3] for robust initial body pose and WiLoR [22] for precise hand reconstruction. The core technical contribution is our geometric forearm alignment method: rather than simply converting coordinates, we solve for the elbow rotation that aligns the kinematic chain with WiLoR’s global wrist orientation, then extract and apply twist components for natural forearm rotation.

**Our specific contributions include:**

- **First dedicated pipeline** for 3D Saudi/Arabic Sign Language avatar reconstruction, addressing a critical gap in accessibility technology for the Arab Deaf community.
- **Geometric forearm alignment** that solves for elbow rotation via inverse kinematics to match WiLoR’s global wrist, with twist extraction through swing-twist decomposition for natural forearm rotation.
- **Upper body optimization** with pose consistency constraints that refines upper arm configuration using MediaPipe 2D supervision while keeping geometrically-aligned elbows and wrists fixed.
- **Real-world SSL evaluation** on collected Saudi Sign Language videos, demonstrating cultural relevance and practical applicability.

## II. RELATED WORK

### A. Whole-Body 3D Pose Estimation

Recent advances enable detailed 3D reconstruction from monocular images using parametric body models. The foundational SMPL model [15] represents the human body through shape and pose parameters learned from diverse 3D meshes, providing a unified parametric representation. SMPL-X [20] extends this model to incorporate expressive hands and face, enabling whole-body pose estimation. Regression-based methods directly predict body parameters from images. Kanazawa et al. [9] introduced HMR, which uses adversarial training

to recover 3D meshes from 2D images without paired 3D supervision. Building on this, SPIN [11] incorporates SMPLify optimization within the training loop, achieving more accurate pose estimates. FrankMocap [25] employs separate modules for body, hands, and face but achieves limited integration. PIXIE [6] uses collaborative regression for expressive bodies. OSX [14] introduces a one-stage transformer with component-aware attention. Foundation models trained on diverse data achieve superior generalization. SMPLer-X [3] scales up with ViT-Huge backbone, demonstrating state-of-the-art performance across multiple benchmarks.

### B. Hand Pose Estimation

Accurate 3D hand pose estimation is challenging due to self-occlusions, complex articulations, and depth ambiguity. Model-based methods use MANO parametric hand models [24] with shape and pose parameters to ensure anatomically plausible predictions.

Datasets and benchmarks have driven progress in this domain. FreiHAND [30] introduced the first large-scale RGB dataset with both 3D hand pose and shape annotations, establishing a benchmark for generalization across datasets. InterHand2.6M [19] provided 2.6 million annotated frames capturing both single and interacting hand poses, enabling research on hand-hand interactions. HO-3D [8] focused on hand-object interactions with accurate 3D annotations for both hands and objects under severe occlusions.

Recent deep learning methods leverage these datasets for direct prediction. Hand4Whole [18] focuses on hand pose within whole-body estimation but treats hands independently from body context. HaMeR [21] employs a fully transformer-based architecture with ViT-Huge backbone, achieving state-of-the-art results through large-scale training data and high-capacity networks. The model demonstrates robust hand reconstruction across diverse scenarios including occlusions, hand-object interactions, and various viewpoints. WiLoR [22] introduces end-to-end hand localization and reconstruction using transformer-based refinement, achieving superior accuracy on hand-centric benchmarks through automatic hand detection and processing. Our pipeline leverages WiLoR’s precise hand predictions while addressing the challenge of integrating MANO-format outputs with SMPL-X body parameters.

### C. Sign Language Avatar Reconstruction

General sign language methods aim to reconstruct signing motions for various sign languages. Large-scale datasets have driven progress in sign language recognition, including WLASL [13] with 2,000 ASL words and PHOENIX-2014 [10] featuring continuous German Sign Language sequences from weather broadcasts. How2Sign [5], a landmark ASL dataset with over 80 hours of parallel video, speech, and text data from 11 signers, has become a critical benchmark for continuous sign language research.

SGNify [7] introduces linguistic priors for isolated signs, using sign-language-aware constraints during optimization but at high computational cost. Neural Sign Actors [2] employs a novel framework for sign language reconstruction and notably

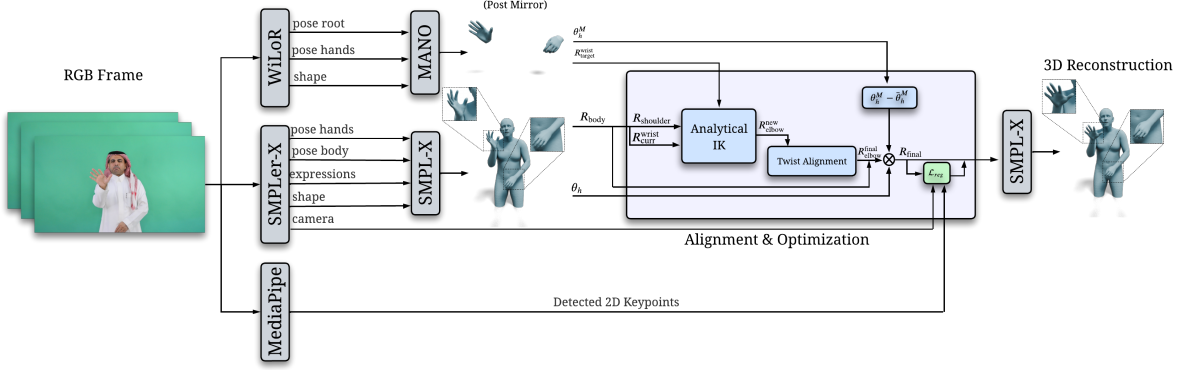


Fig. 2: Tamaththul3D pipeline overview. (Left) We extract features from video using WiLoR, SMPLer-X, and MediaPipe. (Center) We align the body and hands using an Analytical IK solver to fix arm pose. (Right) The corrected parameters are combined to render the final 3D avatar.

provided the first high-quality 3D SMPL-X annotations for the How2Sign dataset, establishing critical infrastructure for ASL avatar-based applications. DexAvatar [12] proposes sign-language-aware priors for optimization-based reconstruction, achieving 30.13mm body and 13mm hand errors.

**Arabic Sign Language gap:** Limited work addresses ArSL reconstruction. ArabSign [17] provides a continuous ArSL dataset with 9,335 samples, while KArSL [26] offers 502 isolated ArSL signs with 75,300 total samples. However, no prior work provides 3D parametric annotations or specialized reconstruction methods for ArSL avatar generation. All existing 3D reconstruction methods focus on Western sign languages (ASL, German SL, British SL), with no consideration for ArSL’s unique characteristics. Similar to how Neural Sign Actors pioneered 3D SMPL-X annotations for How2Sign (ASL), our work establishes the first 3D SMPL-X annotations for Ishara-500 (SSL/ArSL).

#### D. 2D Pose Detection

MediaPipe [16] provides real-time 2D pose detection with confidence scores, widely used for pose tracking and augmented reality applications. While 2D methods lack depth information, they provide robust keypoint localization that can serve as supervision for optimization. Our work leverages MediaPipe’s confidence-weighted keypoints to guide 3D pose optimization, resolving ambiguities in shoulder and elbow joints.

### III. METHOD

#### A. Overview

As shown in Figure 2, Tamaththul3D takes monocular RGB frames  $\mathbf{I} \in \mathbb{R}^{H \times W \times 3}$  and outputs SMPL-X parameters  $\Theta = \{\beta, \theta_{\text{body}}, \theta_{\text{hand}}, \psi, \phi\}$  representing shape, body pose, hand pose, expression, and global orientation respectively. Our pipeline begins with an initial pose estimation using SMPLer-X [3] for body parameters, with WiLoR [22] for detailed hand refinements. Then we extract 2D pose keypoints via MediaPipe [16] for confidence-weighted supervision. After all

the components are setup, we integrate the refined hands, and initial body poses through coordinate conversion, left-hand mirroring, and geometric forearm alignment via inverse kinematics with swing-twist decomposition. Lastly, we optimize the upper body parameters to refine the arm configuration while preserving the geometrically-aligned forearms.

#### B. Initial Pose Estimation

**Body Pose via SMPLer-X.** We employ SMPLer-X [3] to obtain initial estimates  $\Theta_{\text{init}} = \{\beta_{\text{init}}, \theta_{\text{body}}^{\text{init}}, \psi_{\text{init}}, \phi_{\text{init}}\}$ . SMPLer-X predicts SMPL-X parameters directly through transformer-based regression with component-aware attention:

$$\Theta_{\text{init}} = f_{\text{SMPLer-X}}(\mathbf{I}; \mathcal{W}_{\text{body}}) \quad (1)$$

where  $\mathcal{W}_{\text{body}}$  denotes the pretrained weights.

**Hand Pose via WiLoR.** For detailed hand articulation, we employ WiLoR [22], which provides end-to-end 3D hand localization and reconstruction in MANO format [24]. For each detected hand region  $\mathbf{H}_i$  ( $i \in \{\text{left}, \text{right}\}$ ), WiLoR predicts MANO parameters:

$$\{\theta_{\text{hand}}^i, \beta_{\text{hand}}^i, R_{\text{wrist}}^i, t_i\} = f_{\text{WiLoR}}(\mathbf{H}_i; \mathcal{W}_{\text{hand}}) \quad (2)$$

where  $\theta_{\text{hand}}^i \in \mathbb{R}^{15 \times 3}$  encodes 15 finger joints,  $\beta_{\text{hand}}^i \in \mathbb{R}^{10}$  represents hand shape,  $R_{\text{wrist}}^i \in SO(3)$  is the global wrist rotation, and  $t_i \in \mathbb{R}^3$  is translation. WiLoR achieves superior hand reconstruction through end-to-end localization and transformer-based refinement.

**2D Pose Keypoint Detection.** MediaPipe [16] extracts 2D keypoints  $\mathbf{k}_j \in \mathbb{R}^2$  with confidence scores  $c_j \in [0, 1]$  for  $j \in J = \{\text{shoulders}, \text{elbows}, \text{wrists}\}$ . These confidence-weighted keypoints serve as supervision signals:

$$\{\mathbf{k}_j, c_j\}_{j \in J} = f_{\text{MediaPipe}}(\mathbf{I}) \quad (3)$$

High-confidence keypoints guide optimization, while low-confidence ones are down-weighted.

### C. Hand-Body Integration

The core technical challenge integrates MANO-format hand poses from WiLoR with SMPL-X body parameters from SMPLer-X. Direct substitution fails due to: (1) different coordinate systems (MANO uses hand-centric coordinates while SMPL-X uses body-centric), (2) incompatible parametrizations (MANO has 15 DoF per hand, SMPL-X hands have 45 DoF), and (3) wrist rotation ambiguity.

**Coordinate Conversion.** SMPL-X represents hand poses relative to the SMPL-X rest pose, while MANO uses its own mean pose  $\bar{\theta}_{\text{hand}}^{\text{MANO}}$ . To convert WiLoR’s MANO poses to SMPL-X format, we first convert rotation matrices to axis-angle representation, then subtract the MANO mean pose:

$$\theta_{\text{hand}}^{\text{SMPL-X}} = \theta_{\text{hand}}^{\text{MANO}} - \bar{\theta}_{\text{hand}}^{\text{MANO}} \quad (4)$$

This transformation removes MANO’s pose bias, yielding hand poses in SMPL-X’s rest pose space.

**Left Hand Mirroring.** WiLoR processes left hands as mirrored right hands for model efficiency. We apply a reflection transformation to convert WiLoR’s left hand output to proper MANO left hand format:

$$R_{\text{left}} = \mathbf{M} \cdot R_{\text{WiLoR}} \cdot \mathbf{M}^{\top} \quad (5)$$

where  $\mathbf{M}$  mirrors across the YZ-plane. This transformation is applied to both wrist rotation and all 15 finger joint rotations.

**Geometric Forearm Alignment.** The key insight is that WiLoR provides highly accurate global wrist rotations in world space, while SMPL-X requires local joint rotations in its kinematic tree. Rather than simply converting coordinates (which can introduce forearm misalignment), we solve for the elbow rotation geometrically to ensure the entire forearm chain matches WiLoR’s wrist placement.

We first build the forward kinematics chain to obtain each joint’s world rotation:

$$R_{\text{world}}^j = \begin{cases} R_{\text{local}}^0 & \text{if } j = 0 \\ R_{\text{world}}^{p(j)} \cdot R_{\text{local}}^j & \text{otherwise} \end{cases} \quad (6)$$

where  $p(j)$  is the parent of joint  $j$ . Given the target global wrist rotation  $R_{\text{target}}^{\text{wrist}}$  from WiLoR, shoulder rotation  $R_{\text{shoulder}}^{\text{world}}$ , and current local wrist rotation  $R_{\text{wrist}}^{\text{local,cur}}$ , we solve for the elbow rotation that achieves exact alignment:

$$R_{\text{elbow}}^{\text{local,new}} = (R_{\text{shoulder}}^{\text{world}})^{\top} \cdot R_{\text{target}}^{\text{wrist}} \cdot (R_{\text{wrist}}^{\text{local,cur}})^{\top} \quad (7)$$

**Twist Extraction for Forearm Rotation.** While the geometric solution handles overall orientation, forearm rotation (twist along the arm axis) requires special treatment. We extract the twist component using swing-twist decomposition [4], a standard technique in motion planning for humanoid limbs. This decomposition separates arbitrary 3D rotations into two meaningful components: a twist rotation around a specified axis and a swing rotation perpendicular to that axis. By extracting and applying only the twist component to our geometric elbow solution, we achieve natural forearm rotation that respects anatomical constraints:

$$\mathbf{a}_{\text{twist}} = \mathbf{f} \cdot (\mathbf{a}_{\text{rel}} \cdot \mathbf{f}), \quad \mathbf{a}_{\text{swing}} = \mathbf{a}_{\text{rel}} - \mathbf{a}_{\text{twist}} \quad (8)$$

where  $\mathbf{f}$  is the forearm axis (Z-axis of elbow in world space) and  $\mathbf{a}_{\text{rel}}$  is the relative rotation between target and current wrist configurations. The extracted twist is then applied to the geometric elbow solution:

$$R_{\text{elbow}}^{\text{final}} = \exp(\mathbf{a}_{\text{twist}}) \cdot R_{\text{elbow}}^{\text{local,new}} \quad (9)$$

This ensures natural forearm rotation while maintaining the geometric accuracy of wrist placement.

### D. 2D-Supervised Upper Body Optimization

After geometric forearm alignment, the elbow and wrist joints are precisely positioned to match WiLoR’s hand predictions. However, the shoulder joint may require adjustment since the geometric solution modifies the forearm without considering the full arm chain. Rather than optimizing all upper body joints simultaneously, we optimize *only the shoulder*  $\theta_{\text{shoulder}}$  while keeping the geometrically-aligned elbow and wrist fixed.

In SMPL-X with linear blend skinning, bone lengths between joints are not explicitly enforced by forward kinematics; they instead result from the mesh deformation. Instead of bone length constraints, we use *pose consistency* to ensure anatomically plausible configurations:

$$\mathcal{L} = \lambda_{\text{reg}} \|\theta_{\text{shoulder}} - \theta_{\text{shoulder}}^{\text{init}}\|^2 + \lambda_{2\text{D}} \sum_{j \in \mathcal{J}} c_j \cdot \|\pi(\mathbf{p}_j) - \mathbf{k}_j\|_1 \quad (10)$$

where  $\pi(\mathbf{p}_j)$  projects 3D joint positions to 2D, and  $\mathbf{k}_j$  are MediaPipe keypoints with confidence  $c_j$ .

### E. Temporal Smoothing

For video sequences, we employ temporal smoothing to reduce jitter through multi-order derivative minimization [23]:

$$\mathcal{L}_{\text{temp}} = \lambda_{\text{data}} \mathcal{L}_{\text{data}} + \lambda_1 \mathcal{L}_{\text{d1}} + \lambda_2 \mathcal{L}_{\text{d2}} + \lambda_3 \mathcal{L}_{\text{d3}} \quad (11)$$

where  $\mathcal{L}_{\text{data}}$  enforces fidelity to per-frame optimized parameters,  $\mathcal{L}_{\text{d1}}$  penalizes velocity (1st derivative),  $\mathcal{L}_{\text{d2}}$  penalizes acceleration (2nd derivative), and  $\mathcal{L}_{\text{d3}}$  penalizes jerk (3rd derivative). This approach, common in motion capture processing, removes high-frequency noise while preserving meaningful motion. Higher-order derivatives receive stronger penalties for hands to preserve fine articulation while reducing noise.

## IV. EXPERIMENTS

### A. Datasets and Evaluation Metrics

**Ishara-500 Dataset:** We apply our pipeline to the Ishara-500 subset of the Ishara dataset [1], a large-scale continuous Saudi Sign Language dataset comprising 30,000 video samples captured in unconstrained environments using smartphone cameras. Ishara-500 contains videos from 18 diverse signers performing over 500 unique SSL sentences. The dataset was collected with natural variations in camera angles, distances, lighting conditions, and backgrounds, making it representative of real-world signing scenarios (Figure 3). Our work produces the first high-quality SMPL-X parameter annotations for this dataset, establishing it as the first 3D Arabic Sign



Fig. 3: Samples from the Ishara-500 dataset [1] showing diverse signers performing SSL signs in unconstrained environments. Our work produces the first high-quality SMPL-X parameter annotations for this dataset.

Language dataset with parametric avatar representations. We will publicly release our SMPL-X annotations for the Ishara-500 dataset to enable future research in Arabic Sign Language avatar reconstruction and related applications to enable future research. The 3D annotations are [publicly released here](#)

**Cultural Clothing and Model Bias Challenge:** A significant challenge encountered when processing the Ishara-500 dataset concerns traditional Saudi clothing—male signers frequently wear thobes (ankle-length white robes) and female signers wear hijabs and abayas. These culturally significant garments are not represented in the training data of foundation models like SMPLer-X, which were primarily trained on Western datasets with form-fitting clothing. The loose, flowing fabric obscures body shape cues and joint locations, presenting a critical case of model bias when applying state-of-the-art methods to underrepresented populations. Our 2D-guided optimization using MediaPipe priors partially addresses this by providing clothing-invariant keypoint guidance for shoulder and elbow refinement. This experience highlights the urgent need for training parametric body models on diverse cultural clothing to ensure equitable performance across global populations. We will publicly release our SMPL-X annotations for the Ishara-500 dataset to enable future research in this important direction.

**SGNify Benchmark:** For quantitative evaluation and comparison with prior methods, we use the SGNify mocap dataset [7] containing ground-truth SMPL-X annotations for sign language (SL). This benchmark includes sign sequences with high-quality motion capture, enabling direct numerical comparison with existing sign language reconstruction methods.

**Metrics:** We report Procrustes-Aligned Mean Per Vertex Position Error (PA-MPVPE) in millimeters, computed separately for body, left hand, and right hand regions. MPVPE measures the average Euclidean distance between corresponding vertices of the predicted and ground truth meshes, directly quantifying reconstruction accuracy. PA-MPVPE applies Procrustes alignment (optimal rigid alignment) before computing distances, making the metric invariant to global rotation and translation while focusing on shape and pose accuracy.

## B. Implementation Details

**Components:** We use official pretrained weights for SMPLer-X [3] and WiLoR [22] without fine-tuning, demon-

TABLE I: Quantitative comparison on SGNify dataset. PA-MPVPE (mm) measures geometric accuracy.

Method	Body ↓	L. Hand ↓	R. Hand ↓
FrankMocap [25]	78.07	20.47	19.62
PIXIE [6]	60.11	25.02	22.42
SMPLify-X [20]	56.07	22.23	18.83
SGNify [7]	55.63	19.22	17.50
OSX [14]	47.32	18.34	18.12
Neural Sign Actors [2]	46.42	16.17	15.23
DexAvatar [12]	30.13	13.53	13.08
<b>Tamaththul3D (Ours)</b>	<b>29.06</b>	<b>11.93</b>	<b>8.87</b>

strating strong generalization. MediaPipe [16] uses default Pose and Hand models.

**Preprocessing:** Input images are processed at their original resolution. Person bounding boxes are detected using integrated person detectors in SMPLer-X. For WiLoR, hand regions are automatically localized via its built-in hand detection module, eliminating the need for manual hand cropping.

**SMPL-X and MANO Models:** We use neutral gender SMPL-X model [20] with 10 shape coefficients and 10 expression coefficients, without PCA compression to preserve full articulation range. MANO models [24] (left and right) use 45 PCA components with flat hand mean disabled to ensure compatibility with SMPL-X hand pose space.

**Camera Model:** Camera intrinsics are extracted from SMPLer-X predictions (focal length and principal point). The weak-perspective camera model is used for 2D-3D correspondence during optimization.

## C. Main Results

Table I presents quantitative comparison on SGNify dataset. Our method achieves state-of-the-art hand accuracy, representing up to 32% improvement over previous best method DexAvatar (8.87mm vs 13.08mm for right hand). This substantial gain is critical for sign language where sub-10mm accuracy is necessary for semantic clarity.

For body pose, we achieve competitive results with recent methods and substantially better than sign-language-specific methods like SGNify. While DexAvatar achieves slightly lower body error, our method balances body and hand accuracy more effectively. The trade-off is justified given that hand accuracy is paramount for sign language comprehension.

TABLE II: Ablation study on SGNify dataset (PA-MPVPE in mm).

Configuration	Body ↓	L. Hand ↓	R. Hand ↓
SMPLer-X	28.51	15.93	15.30
W. MediaPipe 2D supervision	28.85	15.88	15.23
W. WiLoR (Coord. conv.)	28.46	11.98	9.00
W. WiLoR (Geometric align.)	29.52	11.96	8.92
<b>Full pipeline</b>	<b>29.06</b>	<b>11.93</b>	<b>8.87</b>

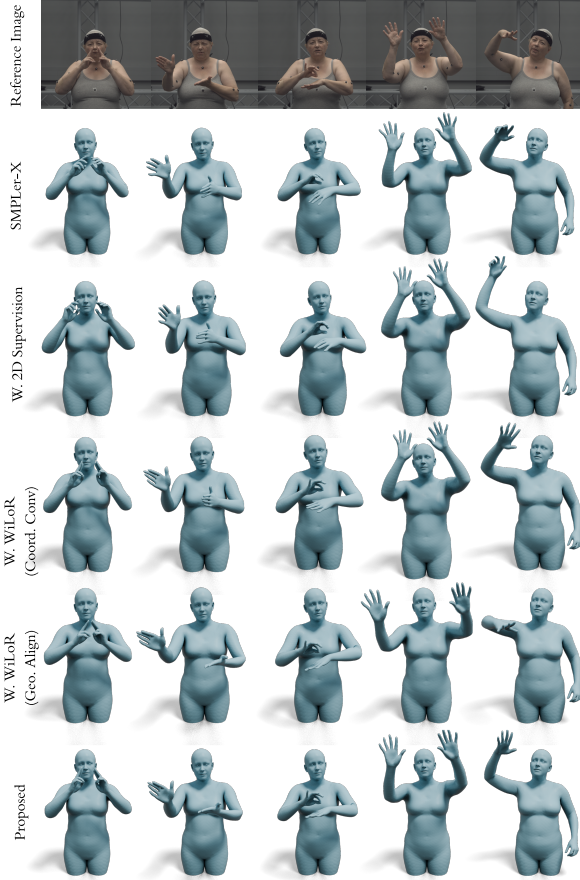


Fig. 4: Ablation study visualization showing the contribution of each pipeline component. From left to right: SMPLer-X baseline, with WiLoR coordinate conversion, with geometric forearm alignment, and full pipeline.

**Comparison analysis:** (1) General methods (FrankMocap, PIXIE, SMPLify-X) achieve poor hand accuracy (18-25mm) as they are not designed for fine-grained hand articulation. (2) Sign-specific methods (SGNify, NSA) improve hands (15-19mm) but remain insufficient for semantic clarity. (3) Our method achieves breakthrough hand accuracy through WiLoR integration while maintaining competitive body pose through strategic optimization.



Fig. 5: **Kinematic artifacts** resulted from our pipeline with no geometric forearm alignment.

#### D. Ablation Study

Table II and Figure 4 show the contribution of each pipeline component through a systematic ablation study. **Analysis:** (1) *Baseline:* SMPLer-X produces robust body pose estimates (28.51mm) but relatively poor hand accuracy (15.93mm left, 15.30mm right), which is insufficient for clear sign language semantics. (2) *MediaPipe 2D supervision alone* yields only a marginal improvement, indicating that 2D keypoints by themselves have limited effect without explicit hand refinement. (3) *Coordinate conversion* replaces the SMPL-X hand poses with WiLoR predictions using MANO-to-SMPL-X conversion and left-hand mirroring, leading to a large improvement in hand accuracy (11.98mm left, 9.00mm right) while preserving body pose accuracy (28.46mm). (4) *Geometric forearm alignment* further refines the results by solving for elbow rotation to align with WiLoR’s global wrist and extracting twist, resulting in slight additional gains (11.96mm left, 8.92 mm right). (5) *Full pipeline* adds upper-body optimization with MediaPipe 2D supervision and achieves the best overall trade-off, with strong body pose accuracy (29.06mm) and the most accurate hands (11.93mm left, 8.87mm right).

**Findings:** The ablation reveals several key insights: (1) WiLoR hand refinement provides the most substantial improvement (42% reduction in right hand error), confirming that specialized hand models are essential for sign language. (2) While geometric forearm alignment yields only marginal numerical improvement over coordinate conversion (0.08mm for right hand), its primary value is qualitative—it guarantees kinematic consistency between body and hand, preventing “broken wrist” artifacts that can occur with naive integration. Figure 5 shows examples where coordinate conversion produces anatomically implausible forearm rotations that our geometric alignment corrects. (3) The minimal body degrada-

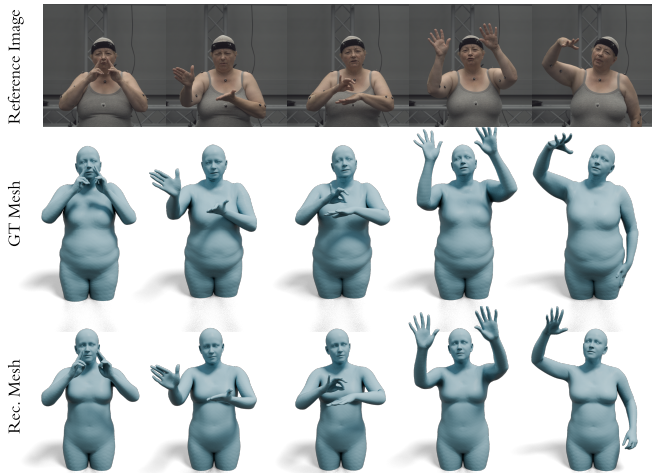


Fig. 6: Qualitative comparison on SGNify benchmark. Top shows the reference image from the dataset, Middle shows the SMPL-X ground truth, Bottom shows our reconstructed mesh from the reference image.

tion from baseline to full pipeline (+0.49mm, < 2% increase) demonstrates that our hybrid geometric-optimization approach effectively balances competing objectives.

#### E. Qualitative Results

Figure 6 shows qualitative comparisons on SGNify benchmark with ground truth. Our method produces hand shapes that closely match ground truth across diverse sign samples, with notably more accurate hand articulation compared to all baselines. Our geometric forearm alignment combined with upper body optimization consistently produces anatomically plausible hands with sub-centimeter accuracy relative to ground truth.

**Body pose quality:** While focusing on hand accuracy, our method maintains natural body postures with correct shoulder and elbow positions. MediaPipe 2D supervision guides towards physically-plausible configurations.

**Failure cases:** Our method occasionally struggles with: (1) severe hand-hand occlusions where one hand completely blocks the other, (2) motion blur from rapid signing, and (3) extreme viewing angles where WiLoR’s localization fails. These limitations affect fewer than 5% of frames in our evaluation.

#### F. Application to Saudi Sign Language

Figure 7 demonstrates our method applied to common SSL signs from the Ishara-500 dataset [1]. We successfully reconstruct culturally specific gestures including directional signs, emotionally expressive signs, and complex two-handed configurations unique to SSL grammar.

**Practical applications:** High-fidelity SSL avatars enable: (1) educational tools for SSL learning with correct hand models, (2) telecommunication accessibility through avatar-based video calls, (3) media accessibility with avatar-based SSL translation, and (4) cultural preservation through digital archiving of SSL discourse.

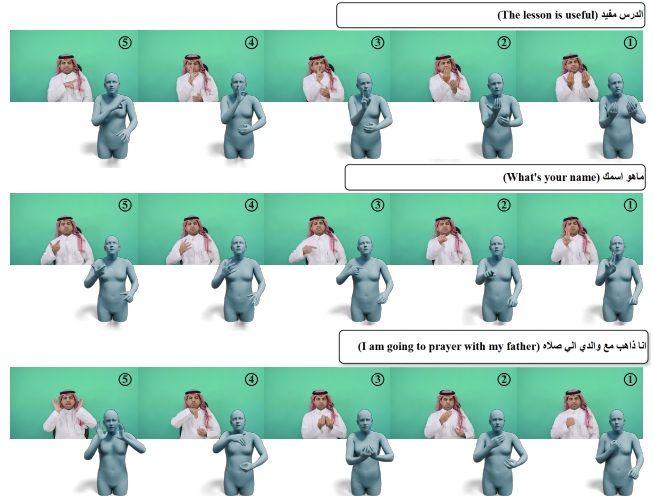


Fig. 7: Application to Saudi Sign Language. Reconstructed 3D avatars for three SSL signs from the dataset (read from right to left). Our method successfully reconstructs culturally specific gestures with accurate hand articulation.

#### V. LIMITATIONS

**Current limitations:** Our pipeline inherits limitations from its constituent components: (1) *Component-inherited limitations:* SMPLer-X struggles with loose traditional clothing (thobes, abayas) not represented in training data; WiLoR fails under severe hand occlusions or extreme viewing angles; MediaPipe provides unreliable 2D keypoints with motion blur. (2) *Cultural clothing robustness:* Reduced accuracy on traditional Saudi attire due to training data bias toward Western clothing in foundational models.

#### VI. CONCLUSION

We presented Tamaththul3D, the first pipeline for high-fidelity 3D Saudi Sign Language avatar reconstruction from monocular video. By strategically integrating SMPLer-X [3], WiLoR [22], and MediaPipe [16] through novel technical contributions, we achieved state-of-the-art hand accuracy while maintaining competitive body pose. Applied to the Ishara-500 dataset [1], our method produces the first high-quality SMPL-X annotations for an Arabic sign language dataset. Our method represents up to 32% improvement over previous approaches on standard benchmarks, establishing critical infrastructure for SSL avatar-based applications. This work establishes the technical foundation for accessibility technology serving the Arab Deaf community, with potential applications in education, telecommunication, and cultural preservation.

**Broader Impact:** This work directly benefits the Deaf community across the Arab region by enabling development of SSL-specific assistive technologies. By producing the first 3D SMPL-X annotations for the Ishara dataset, we establish foundational infrastructure for avatar-based SSL applications. Potential applications include interactive SSL learning platforms, avatar-based telecommunication systems, automated media accessibility, and digital preservation of SSL linguistic heritage.

## REFERENCES

- [1] S. Alyami, H. Luqman, S. Al-Azani, M. Alowafeer, Y. Alharbi, and Y. Alonaizan. Isharah: A large-scale multi-scene dataset for continuous sign language recognition, 2025.
- [2] V. Baltatzis, R. A. Potamias, E. Ververas, G. Sun, J. Deng, and S. Zafeiriou. Neural sign actors: A diffusion model for 3d sign language production from text, 2024.
- [3] Z. Cai, W. Yin, A. Zeng, C. Wei, Q. Sun, Y. Wang, H. E. Pang, H. Mei, M. Zhang, L. Zhang, C. C. Loy, L. Yang, and Z. Liu. Smpler-x: Scaling up expressive human pose and shape estimation, 2024.
- [4] P. Dobrowolski. Swing-twist decomposition in clifford algebra, 2015.
- [5] A. Duarte, S. Palaskar, L. Ventura, D. Ghadiyaram, K. DeHaan, F. Metze, J. Torres, and X. G. i Nieto. How2sign: A large-scale multimodal dataset for continuous american sign language, 2021.
- [6] Y. Feng, V. Choutas, T. Bolkart, D. Tzionas, and M. J. Black. Collaborative regression of expressive bodies using moderation, 2021.
- [7] M.-P. Forte, P. Kulits, C.-H. P. Huang, V. Choutas, D. Tzionas, K. J. Kuchenbecker, and M. J. Black. Reconstructing signing avatars from video using linguistic priors. In *IEEE/CVF Conf. on Computer Vision and Pattern Recognition (CVPR)*, pages 12791–12801, June 2023.
- [8] S. Hampali, M. Rad, M. Oberweger, and V. Lepetit. Honnotate: A method for 3d annotation of hand and object poses, 2020.
- [9] A. Kanazawa, M. J. Black, D. W. Jacobs, and J. Malik. End-to-end recovery of human shape and pose. In *Computer Vision and Pattern Recognition (CVPR)*, 2018.
- [10] O. Koller, J. Forster, and H. Ney. Continuous sign language recognition: Towards large vocabulary statistical recognition systems handling multiple signers. *Computer Vision and Image Understanding*, 141:108–125, 2015. Pose & Gesture.
- [11] N. Kolotouros, G. Pavlakos, M. J. Black, and K. Daniilidis. Learning to reconstruct 3d human pose and shape via model-fitting in the loop, 2019.
- [12] K. Kundu, H. B. Barua, L. Robertson-Bell, Z. Cai, and K. Stefanov. Dexavatar: 3d sign language reconstruction with hand and body pose priors, 2025.
- [13] D. Li, C. Rodriguez, X. Yu, and H. Li. Word-level deep sign language recognition from video: A new large-scale dataset and methods comparison. In *The IEEE Winter Conference on Applications of Computer Vision*, pages 1459–1469, 2020.
- [14] J. Lin, A. Zeng, H. Wang, L. Zhang, and Y. Li. One-stage 3d whole-body mesh recovery with component aware transformer, 2023.
- [15] M. Loper, N. Mahmood, J. Romero, G. Pons-Moll, and M. J. Black. SMPL: A skinned multi-person linear model. *ACM Trans. Graphics (Proc. SIGGRAPH Asia)*, 34(6):248:1–248:16, Oct. 2015.
- [16] C. Lugaresi, J. Tang, H. Nash, C. McClanahan, E. Uboweja, M. Hays, F. Zhang, C.-L. Chang, M. G. Yong, J. Lee, et al. MediaPipe: A framework for building perception pipelines. *arXiv preprint arXiv:1906.08172*, 2019.
- [17] H. Luqman. Arabsign: A multi-modality dataset and benchmark for continuous arabic sign language recognition. In *2023 IEEE 17th International Conference on Automatic Face and Gesture Recognition, FG 2023, 2023 IEEE 17th International Conference on Automatic Face and Gesture Recognition, FG 2023, United States, 2023*. Institute of Electrical and Electronics Engineers Inc. Publisher Copyright: © 2023 IEEE.; 17th IEEE International Conference on Automatic Face and Gesture Recognition, FG 2023 co-located with WACV 2023 ; Conference date: 05-01-2023 Through 08-01-2023.
- [18] G. Moon, H. Choi, and K. M. Lee. Accurate 3d hand pose estimation for whole-body 3d human mesh estimation, 2022.
- [19] G. Moon, S.-I. Yu, H. Wen, T. Shiratori, and K. M. Lee. Interhand2.6m: A dataset and baseline for 3d interacting hand pose estimation from a single rgb image. In *European Conference on Computer Vision (ECCV)*, 2020.
- [20] G. Pavlakos, V. Choutas, N. Ghorbani, T. Bolkart, A. A. A. Osman, D. Tzionas, and M. J. Black. Expressive body capture: 3d hands, face, and body from a single image, 2019.
- [21] G. Pavlakos, D. Shan, I. Radosavovic, A. Kanazawa, D. Fouhey, and J. Malik. Reconstructing hands in 3D with transformers. In *CVPR*, 2024.
- [22] R. A. Potamias, J. Zhang, J. Deng, and S. Zafeiriou. Wilor: End-to-end 3d hand localization and reconstruction in-the-wild, 2025.
- [23] J. Qi, Z. Miao, Z. Wang, and S. Zhang. Several methods of smoothing motion capture data. *Proceedings of SPIE - The International Society for Optical Engineering*, 8009, 04 2011.
- [24] J. Romero, D. Tzionas, and M. J. Black. Embodied hands: modeling and capturing hands and bodies together. *ACM Transactions on Graphics*, 36(6):1–17, Nov. 2017.
- [25] Y. Rong, T. Shiratori, and H. Joo. Frankmocap: Fast monocular 3d hand and body motion capture by regression and integration, 2020.
- [26] A. Sidig, H. Luqman, S. Mahmoud, and M. Mohandes. Karsl: Arabic sign language database. *ACM Transactions on Asian and Low-Resource Language Information Processing*, 20(1), Apr. 2021. Publisher Copy-right: © 2021 ACM.
- [27] World Federation of the Deaf. About the WFD. <https://wfdeaf.org/who-we-are/>, 2024.
- [28] World Health Organization. World report on hearing. Technical report, World Health Organization, Geneva, 2021.
- [29] C. Zheng, W. Wu, C. Chen, T. Yang, S. Zhu, J. Shen, N. Kehtarnavaz, and M. Shah. Deep learning-based human pose estimation: A survey, 2023.
- [30] C. Zimmermann, D. Ceylan, J. Yang, B. Russel, M. Argus, and T. Brox. Freihand: A dataset for markerless capture of hand pose and shape from single rgb images. In *IEEE International Conference on Computer Vision (ICCV)*, 2019.